
Convergence Error Analysis of Reflected Gradient Langevin Dynamics for Globally Optimizing Non-Convex Constrained Problems

Kanji Sato¹, Akiko Takeda^{1,2}, Reiichiro Kawai³, and Taiji Suzuki^{1,2}

¹Graduate School of Information Science and Technology, The University of Tokyo

²Center for Advanced Intelligence Project, RIKEN

³Graduate School of Arts and Sciences, The University of Tokyo

Abstract

Non-convex optimization problems have various important applications, whereas many algorithms have been proven only to converge to stationary points. Meanwhile, gradient Langevin dynamics (GLD) and its variants have attracted increasing attention as a framework to provide theoretical convergence guarantees for a global solution in non-convex settings. The studies on GLD initially treated unconstrained convex problems and very recently expanded to convex constrained non-convex problems by Lamperski (2021). In this work, we can deal with non-convex problems with some kind of non-convex feasible region. This work analyzes reflected gradient Langevin dynamics (RGLD), a global optimization algorithm for smoothly constrained problems, including non-convex constrained ones, and derives a convergence rate to a solution with ϵ -sampling error. The convergence rate is faster than the one given by Lamperski (2021) for convex constrained cases. Our proofs exploit the Poisson equation to effectively utilize the reflection for the faster convergence rate.

1 Introduction

We are interested in the following (generally) non-convex problems over a domain $K \subset \mathbb{R}^d$ defined by

$$\min_{x \in \mathbb{R}^d} f(x) \quad \text{s.t.} \quad x \in K, \quad (1)$$

where $f : \mathbb{R}^d \rightarrow \mathbb{R}$ is a non-convex function and K is a (possibly non-convex) bounded region with smooth boundary. Let us also assume that K are thick enough to contain a Euclidean ball. The assumptions on K and f will be specified in Section 3.1 in detail.

We consider the following *reflected gradient Langevin dynamics (RGLD)* as an optimization algorithm to minimize the non-convex objective on a possibly non-convex feasible region K . The RGLD algorithm is basically the gradient Langevin dynamics (or unadjusted Langevin algorithm) but includes a *reflection step* so that the intermediate solution does not go outside the feasible region:

$$\begin{cases} X'_{k+1} = X_k - \eta \nabla f(X_k) + \sqrt{\frac{2\eta}{\beta}} \xi_{k+1} \\ X_{k+1} = \mathcal{R}_K(X'_{k+1}), \end{cases}$$

where \mathcal{R}_K is the reflection operator defined later in (2), ξ_{k+1} is an i.i.d. Rademacher random vector in \mathbb{R}^d (i.e., each element of which is i.i.d. a Rademacher random variable), $\eta(> 0)$ is the step size, and $\beta(> 0)$ is the inverse temperature parameter. Although it was proved that the continuous-time limit of $\{X_k\}$ converges to a unique stationary distribution (Bubeck et al., 2018), i.e., the Gibbs distribution $\pi(x) \sim \exp(-\beta f(x))$ supported on K , which concentrates around the global minima of $f(x)$ on K , the error analysis of the discrete-time algorithm has not been extensively explored yet. The main purpose of this work is to give the error analysis including the convergence rate and the discretization error of the discrete-time RGLD algorithm to optimize the problem (1).

		objective function	
		convex	non-convex
unconstrained		Dalalyan (2017) $\tilde{O}(\epsilon^{-2})$	Zou et al. (2021) $\tilde{O}(d^4\epsilon^{-2})$
constrained	convex	Hsieh et al. (2018) $\tilde{O}(d\epsilon^{-2})$	Lamperski (2021) $\tilde{O}(d^4\lambda_*^{-1}\epsilon^{-4})$
	non-convex	This work $\tilde{O}(d^3\lambda_*^{-3}\epsilon^{-3})$	

Table 1: Iteration complexity of gradient Langevin dynamics to converge to the Gibbs distribution π . \tilde{O} is the order ignoring polylogarithmic factors. λ_* is the spectral gap.

Non-convex optimization has been essential in many machine learning applications such as tensor factorization (Signoretto et al., 2013; Suzuki et al., 2016), robust classification using non-convex losses (Masnadi-shirazi and Vasconcelos, 2009), deep learning (Kingma and Ba, 2014). While unconstrained problems have been widely studied in various contexts, constrained problems also emerge in many important applications such as portfolio optimization (Barkhagen et al., 2019) and sparse estimation with non-convex regularization (Wen et al., 2018; Zhang et al., 2018). However, the existence of constraints sometimes complicates the problems, which leads to deteriorated computational efficiency. While various algorithms have been proposed to solve constrained problems (Li and Lin (2015); Xie and Wright (2021); Hinder and Ye (2018); Lin et al. (2019)), many of them are proposed to achieve first-order optimality and thus their theoretical analyses are limited to proving convergence to stationary points since non-convex optimization is known to be difficult to globally optimize in general.

However, a line of works on Langevin dynamics, originating from stochastic diffusions, has focused on global optimization of non-convex problems in limited situations, where the objective function is required to be smooth to some extent (Geman and Hwang, 1986; Chiang et al., 1987; Gelfand and Mitter, 1991). The algorithms appearing in these works are often called gradient Langevin dynamics (GLD). Nevertheless, constrained non-convex problems have not been analyzed until very recently because of the theoretical difficulties of the underlying stochastic differential equations (SDE); even proving the existence of the solution of the underlying SDE is non-trivial (see Tanaka (1979); Lions and Sznitman (1984)). Very recently, Lamperski (2021) analyzed projected gradient Langevin dynamics (PGLD), proposed by Bubeck et al. (2018), for convex constrained non-convex problems and gave its convergence rate. However, his work does not cover non-convex constraints and leaves a gap between the obtained convergence rates in the unconstrained setting and that in the constrained one (see Table 1).

Our Contributions This paper focuses on enriching the theoretical analysis of constrained optimization problems, especially those having (generally non-convex) smooth constraints, by considering the RGLD algorithm.

While Lamperski (2021) adopted a coupling argument for the 1-Wasserstein metric with the convexity assumption of the feasible region K and showed geometric ergodicity, its time discretization error was $O((\eta \log k)^{1/4})$ which is slower than the unconstrained counterpart $O(\eta^{1/2})$ in terms of the convergence with respect to the 1-Wasserstein metric. This is mainly because they employed the projected gradient Langevin dynamics (PGLD) and gave the rough estimate of the discretization error by the convergence in mean. Although PGLD has already been equipped with a convergence guarantee for the convex-constrained problems (e.g., Bubeck et al. (2018)), it induces a suboptimal rate.

To overcome this difficulty, we replace the projection step with a so-called “reflection” step to keep the trajectory inside the feasible region. Indeed, this strategy enables us to give a better convergence guarantee by canceling out a certain error term. Although the reflection step incurs further theoretical difficulties, we exploit the Poisson equation of the corresponding continuous-time dynamics as in Leimkuhler et al. (2020), which yields a simpler proof by adopting some known results on the dynamics. Moreover, we explicitly specify the parameter dependence of the error bound to derive the convergence rate, which was not covered by Leimkuhler et al. (2020, Theorem 4.2). This is important because the optimization requires employing a large inverse temperature β , and thus the dependence on β and d is of great interest in optimization problems. As shown in Table 1, our proven convergence rate is sharper than that of Lamperski (2021) thanks to the better discretization error while there remains a gap between the best known rate under unconstrained formulations and that under constrained ones.

Moreover, this is the first work to address non-convex constrained situations, requiring a certain smoothness assumption on the feasible region, which has not been imposed so far (e.g., by Lamperski (2021)).

Related Works on GLD GLD, including its stochastic variant (SGLD), has been studied for a long time, starting with Geman and Hwang (1986). It has also been studied in the context of Bayesian learning, for instance, by Welling and Teh (2011). Chiang et al. (1987); Gelfand and Mitter (1991), and their following works examined the convergence of GLD to the global minimum of the objective functions, whereas Zhang et al. (2017) obtained the convergence to local optima.

Taking advantage of the accumulated probabilistic analyses of GLD and SGLD, Raginsky et al. (2017); Xu et al. (2018); Vempala and Wibisono (2019) proved a non-asymptotic convergence rate to global optima by analyzing GLD for unconstrained non-convex problems. Zou et al. (2021) is the best known work that provides the fastest convergence rate. A line of studies has extended the conventional GLD to its variants. Chen et al. (2021) combined SGLD with the stochastic variance-reduced gradient (SVRG), while Durmus et al. (2018) worked on a non-smooth objective function by making use of the Moreau envelope.

Among such varied researches, Bubeck et al. (2018) is considered to be the first known work that analyzed projected gradient Langevin dynamics (PGLD) for constrained sampling. They aimed to sample from a log-concave distribution, which translates to convex optimization in our context. Brosse et al. (2017) also focused on sampling from a constrained log-concave distribution by utilizing a proximal operation. Proximal-type algorithms are also considered in Pereyra (2016); Salim et al. (2019); Salim and Richtarik (2020). Hsieh et al. (2018); Zhang et al. (2020b) proposed mirrored Langevin dynamics as a way to handle constraints. They used the mirror map to transform the target distribution into an unconstrained one, to which many existing methods can be applied. Finding an appropriate mirror map is a non-trivial task in practice, though. Patterson and Teh (2013); Wang et al. (2020) can be located in the context of constrained optimization when the feasible region forms a Riemannian manifold such as the Stiefel manifold or the Grassmann manifold.

Parpas et al. (2006) firstly proposed a GLD algorithm that converges to the global optimum for linearly constrained non-convex problems. Very recently, Lamperski (2021) proved a non-asymptotic convergence rate of PGLD for convex constrained non-convex problems. The key components of the theoretical analysis are reflected stochastic differential equations (RSDE) and their discretization, which are also essential for our analysis.

Tanaka (1979); Lions and Sznitman (1984) discussed the existence and uniqueness of solutions of reflected diffusions, named the “Skorokhod problem”. Dupuis and Ramanan (1999); Andres (2011) studied the regularity of the solutions, and Banerjee and Budhiraja (2020); Freidlin (1985) present the existence of a unique invariant measure of RSDEs. RSDEs have been analyzed from the viewpoint of partial differential equations (PDE), for instance, by Miranda (1970); Cerrai (1998); Barbu and Prato (2005). The discretization error of RSDEs has been a key component to connect the analysis on SDEs with the convergence rate to optimization algorithms; Leimkuhler et al. (2020); Cattiaux et al. (2017); Ding and Zhang (2008) studied this aspect.

2 Our Proposed Algorithm: RGLD

Here, we describe the details of the reflected gradient Langevin dynamics (RGLD) method. To properly describe the algorithm, we define some notations.

Notation We call a random variable ξ a Rademacher random variable if it satisfies $\mathbb{P}(\xi = +1) = \mathbb{P}(\xi = -1) = 1/2$, and call a vector-valued random variable a Rademacher random vector if each element of the vector is an independent Rademacher random variable. For a compact set $K \subset \mathbb{R}^d$, we define the projection \mathcal{P}_K and reflection \mathcal{R}_K respectively as

$$\mathcal{P}_K(x) := \arg \min_{y \in K} \|y - x\|, \quad \mathcal{R}_K(x) := 2\mathcal{P}_K(x) - x. \quad (2)$$

Let ∂K , K° , K^c and \bar{K} denote the boundary, interior, complement and closure of K respectively. Denote by $K_{-r'}$ the set of the points outside K whose distance from K are at most $r' > 0$. $\tilde{\mathcal{O}}$ represents the order symbol ignoring the poly-log arithmetic factors, that is, for sequences (f_n) and (g_n) , $f_n = \tilde{\mathcal{O}}(g_n)$ means that there exists constants $C, c > 0$ such that $|f_n| \leq C|g_n| \log^c(|g_n|)$ for all n . Similarly, we write $f \preceq g$ for positive functions f and g if there exists a constant $C > 0$ such that $f \leq Cg$, and write $f \sim g$ if $f \preceq g \wedge f \succeq g$. Finally, we let $[n] := \{0, 1, \dots, n-1\}$.

The most common approach to a constrained optimization problem would be the projected gradient descent (PG), the procedure of which is given by

$$X_{k+1} = \mathcal{P}_K(X_k - \eta \nabla f(X_k)).$$

However, PG may well be stuck on a saddle point or a suboptimal local optimal solution. To escape from such a globally suboptimal critical point, it is helpful to add a stochastic perturbation. The gradient Langevin dynamics (GLD)

is one of the most common approaches in that direction (Welling and Teh, 2011; Raginsky et al., 2017). To adapt GLD to a constrained optimization problem, GLD is combined with the projected operation as in the projected GLD (PGLD) algorithm and its theoretical property has been analyzed especially with a convex constraint (Bubeck et al., 2018; Lamperski, 2021). Conventionally, Gaussian noise is used to approximate the Brownian motion term appearing in the continuous-time counterpart of GLD but it sometimes creates so huge a noise that the solution moves far away from the feasible region. Therefore, we employ the Rademacher random vector instead of the Gaussian noise perturbation to keep the solution close to the domain since a Rademacher random variable is bounded.

While the projection step has been commonly used to keep the feasibility condition, we employ the reflection operation instead because we find that it can cancel out the second-order term in the discretization error analysis and achieves higher-order approximation error, which will be fully discussed in Appendix C.1. This is analogous to the fact that the reflection step in the Douglas-Rachford algorithm speeds up convergence in the feasibility problem as shown in Artacho et al. (2020). Keeping these notions in our mind, we arrive at the following RGLD method which is analyzed in this paper.

Algorithm 2.1 (Reflected gradient Langevin dynamics (RGLD)).

$$\begin{cases} X'_{k+1} = X_k - \eta \nabla f(X_k) + \sqrt{\frac{2\eta}{\beta}} \xi_{k+1} \\ X_{k+1} = \mathcal{R}_K(X'_{k+1}), \end{cases}$$

where $\eta > 0$ and $\beta > 0$ are the step size and the inverse temperature parameter respectively, and ξ_k is an i.i.d. Rademacher random vector in \mathbb{R}^d .

Note that the boundedness of the Rademacher noise assures that the reflection is uniquely defined for every iteration even if the domain is non-convex when the boundary of the feasible region is sufficiently smooth. One has to reject a huge increment by the Gaussian noise as in Bossy et al. (2004), which could degrade the convergence.

RGLD algorithm (Algorithm 2.1) can be viewed as a time-discretized version of the continuous-time reflected gradient Langevin diffusion described by

$$dX_t = -\nabla f(X_t)dt + \sqrt{\frac{2}{\beta}}dW_t - v(X_t)L(dt), \quad (t \geq 0), \quad (3)$$

where (W_t) is the standard d -dimensional Brownian motion, $v(X_t)$ is an outer unit normal vector at X_t , and L is the local time supported on the set $\{t \in \mathbb{R}_+ \mid X_t \in \partial K\}$. Here, we say that $v(x)$ is an outer unit normal vector at $x \in \partial K$ if $\|v(x)\| = 1$ and there exists $\epsilon > 0$ such that

$$x' \in K \text{ satisfies } \|x - x'\| < \epsilon \Rightarrow \langle x - x', v(x) \rangle \geq 0.$$

We note that $v(x) = \mathbf{0}$ is the outer unit normal vector for $x \in K^\circ$, and thus RGLD is reduced to the standard gradient Langevin dynamics on K° . We notice that there exists the reflection term $-v(X_t)L(dt)$ which is required to cancel out the velocity directed to outside the region, as thoroughly discussed in Tanaka (1979); Lions and Sznitman (1984); Dupuis and Ramanan (1999). This term imposes a non-trivial treatment when we discretize the dynamics. Indeed, there are at least two choices, projection or reflection, to implement in the discrete-time setting.

According to Bubeck et al. (2018), it is known that under suitable conditions, the continuous-time RGLD (3) weakly converges to a unique stationary distribution, the Gibbs distribution with the density function π defined by

$$\pi(x) = \frac{\exp(-\beta f(x))}{\int_K \exp(-\beta f(y))dy} \quad (x \in K), \quad (4)$$

and $\pi(x) = 0$ for $x \notin K$. This explicit representation of the Gibbs distribution enables us to bound the discrepancy between the expectation of the objective with respect to the stationary distribution and the optimal value as usual (Raginsky et al., 2017). Our main strategy is to show the weak convergence of the discrete-time dynamics to the stationary distribution by bounding the discretization error through the Poisson equation.

3 Convergence Analysis

In this section, we state the main theorem on the convergence rate of RGLD under the assumptions given in Section 3.1 and give a sketch of its proof.

3.1 Assumptions

First, we prepare the assumptions on K and f for our convergence analysis.

Assumption 3.1 (Conditions on K).

1. \mathcal{P}_K is efficiently computable by some oracle as long as it is unique.
2. $K \subset \mathbb{R}^d$ is the closure of a possibly non-convex open and connected domain such that $0 \in K$ and, as a consequence, K contains a Euclidean ball of radius r .
3. K has a smooth boundary such that $\partial K \in C^4$.
4. K is bounded; that is, K is included in a sphere of radius R centered at the origin.
5. The problem (1) admits at least one optimal solution $x^* \in K$.

Assumption 3.1.1 is required to ensure that the reflection step in our algorithm can be easily computed. Assumption 3.1.2 is necessary to guarantee the uniqueness of the invariant law of the reflected diffusion process (3) (Miranda, 1970; Benchérif-Madani and Pardoux, 2009), which is a key component of the global optimization of RGLD. Moreover, it also allows a reflection operation lest the operation moves the solution outside the domain again. Assumption 3.1.3 is a relatively strict condition because many constrained problems have multiple constraints and, thus, may have several indifferentiable extreme points. An example of a domain with a smooth boundary is a thick-walled sphere (Chepurnenko et al., 2021; Zhang et al., 2020a). A Riemannian manifold such as the Stiefel manifold or the Grassmann manifold, also satisfies the assumptions, covered by some of the existing works (Patterson and Teh, 2013; Wang et al., 2020). The l_q norm ($q < 1$) is one of the most popular non-convex constraints for sparse estimation but it violates Assumption 3.1.3 at points with zero elements. However, by applying some smoothing operation, we may also make it have a smooth boundary.

Next, we describe the assumption on f .

Assumption 3.2 (Conditions on f).

1. f is a C^4 function.
2. ∇f is accessible by some oracle.

From these assumptions, we can conclude that f and the norm of ∇f are bounded by a constant G because the feasible region K is compact. Moreover, M -smoothness of the objective function is easily established.

Proposition 3.3. *Under Assumptions 3.1.4 and 3.2.1, there exists a constant $M > 0$ such that f is M -smooth, that is, for any $x, y \in K$, it holds that $\|\nabla f(x) - \nabla f(y)\| \leq M\|x - y\|$.*

Under these assumptions, we can confirm that the reflection is unique for sufficiently small η . Indeed, we can show $\|\mathcal{P}_K(X'_k) - X'_k\| = O(\eta + \sqrt{d\eta/\beta})$, which is sufficient to ensure the uniqueness under Assumption 3.1.3 (See Bossy et al. (2004); Leimkuhler et al. (2020) for a more thorough statement). Then, under Assumption 3.1.2, we can guarantee $\mathcal{R}_K(X'_k) \in K$ for sufficiently small η , which confirms the well-definedness of RGLD.

3.2 Main Result: Convergence Rate of RGLD

Here, we give our main result about the convergence rate of RGLD. In our analysis, we utilize the geometric ergodicity of the continuous-time RGLD. The rate of its weak convergence to the unique invariant measure is governed by the spectral gap λ_* defined by

$$\lambda_* := \inf_{\phi \in W^{1,2}(K^o), \phi \neq 0} \frac{\int_K \|\nabla \phi\|^2 d\pi}{\beta \int_K \phi^2 d\pi}, \quad (5)$$

where $W^{1,2}(K^o)$ is the Sobolev space such that the function itself and its weak derivative have finite L^2 norms on K^o . Note that λ_* is the smallest, or the principal, eigenvalue of the infinitesimal generator of (X_t) which is studied in, for example, Chen and Lou (2012); Peng et al. (2019).

Under this preparation, we obtain the following rate of convergence.

Theorem 3.4 (Main Theorem). *Suppose that Assumptions 3.1 and 3.2 hold. Then, for any $\beta > 0$, the following bound holds*

$$\mathbb{E} \left[\min_{k \in [N]} f(X_k) \right] - \min f \leq C \left(\frac{1}{\lambda_* N \eta} + \frac{\sqrt{\eta} (\beta \sqrt{\eta} + (\beta \eta + d)^{3/2})}{\lambda_*} + \frac{d}{\beta} \log \beta \right),$$

where $C > 0$ is a constant independent of $\lambda_*, N, \eta, \beta, d$. In particular, for any $0 < \epsilon \ll 1$, by setting each parameter as

$$\beta > 0, \eta \leq \min \left\{ \frac{\lambda_*^2 \epsilon^2}{d^3}, \frac{\lambda_* \epsilon}{\beta} \right\}, N \geq \frac{1}{\lambda_* \epsilon \eta} \geq \max \left\{ \frac{d^3}{\lambda_*^3 \epsilon^3}, \frac{\beta}{\lambda_*^2 \epsilon^2} \right\},$$

we have

$$\mathbb{E} \left[\min_{k \in [N]} f(X_k) \right] - \min f \leq \epsilon + \frac{d \log \beta}{\beta}.$$

Informally speaking, the main theorem states that, by selecting a sufficiently small η , an ϵ -sampling error is achieved after $\tilde{O}(\max\{d^3 \lambda_*^{-3} \epsilon^{-3}, \beta \lambda_*^{-2} \epsilon^{-2}\})$ iterations of RGLD. Now, remember that the iteration complexity for the PGLD obtained by the previous work (Lamperski, 2021) was evaluated as $N = \tilde{O}(d^4 \lambda_*^{-1} \epsilon^{-4})$ (see Table 1). This is worse than our evaluation $N = \tilde{O}(d^3 \lambda_*^{-3} \epsilon^{-3})$ when β is sufficiently large as $\beta = \tilde{\Omega}(d)$ (which is the situation of the interest).

This advantage is mainly due to the employment of the reflection operator instead of the projection. The discretization error can be evaluated by approximating the time differentiation for the infinitesimal generator by a discrete-time differentiation and in that approximation, we can cancel out the second-order derivatives thanks to the symmetric relation between X_k and X'_k . Hence, we obtain a sharper bound than that of PGLD. On the other hand, Lamperski (2021, Lemmas 5, 6) showed that the discretization error between $f(X_k)$ and $f(X_{k\eta})$ is $\tilde{O}(\eta^{1/4})$ which is worse than our analysis. Although we might be able to improve the rate even for PGLD, it would require ensuring the hitting time on the boundary is negligibly small so that the difference of projection and reflection could be ignored. Another reason of the suboptimality is the crude estimate of 1-Wasserstein metric by the pathwise distance $\mathbb{E}[\|X_k - X_{k\eta}\|]$, which should be less tight than the direct evaluation of the difference in a weak convergence sense. We cope with this issue by exploiting the solution of the corresponding Poisson equation.

Remark 3.5. The dependence of λ_* on β is an open problem and has been studied in Chen and Lou (2012); Peng et al. (2019). λ_* is supposed to be proportional to the exponential of β since the exponential dependence is proved for unconstrained GLD under the similar assumptions in Raginsky et al. (2017); Gayrard et al. (2005); Bardet et al. (2018). If that is true, the task of finding an ϵ -optimal solution suffers from the curse of dimensionality, where ϵ -optimal solution x is defined as the solution which satisfies $\mathbb{E}[f(x)] - \min_K f \leq \epsilon$. Indeed, it is necessary to set $\beta \geq d\epsilon^{-1} \log \epsilon^{-1}$ to assert $\mathbb{E}[\min_{k \in [N]} f(X_k)] - \min_K f \leq \epsilon$. A simple calculation shows that this implies $N \geq \exp(c_1 d \epsilon^{-1})$. N depends on both the exponential of the dimensionality d and that of the inverse of the admitted error ϵ .

3.3 Proof Sketch of Theorem 3.4

In this subsection, we give a proof sketch of Theorem 3.4. We will denote any constant independent of $\lambda_*, N, \eta, \beta, d$ by the same notation C for simplicity. Theorem 3.4 immediately follows from the following lemma by noticing $\min_{k \in [N]} f(X_k) \leq \frac{1}{N} \sum_{k=0}^{N-1} f(X_k)$.

Lemma 3.6. Under Assumptions 3.1 and 3.2, if $\beta > 0$, then it holds that

$$\mathbb{E} \left[\frac{1}{N} \sum_{k=0}^{N-1} f(X_k) \right] - \min f \leq C \left(\frac{1}{\lambda_* N \eta} + \frac{\sqrt{\eta} (\beta \sqrt{\eta} + (\beta \eta + d)^{3/2})}{\lambda_*} + \frac{d}{\beta} \log(C\beta) \right).$$

Given this evaluation, we can easily obtain the parameter configuration in Theorem 3.4 to obtain a solution with ϵ -sampling error by controlling the first two terms on the right-hand side to make them smaller than ϵ . For completeness, we attach the proof of Theorem 3.4 from Lemma 3.6 in Appendix A.

Hereafter, we give a proof of Lemma 3.6. Recall that the algorithm $\{X_k\}$ is a time-discretized version of the continuous-time version (X_t) following the SDE (3). One finds that (X_t) geometrically converges in distribution to the Gibbs distribution π given in (4) (see Lemma C.4). It can be shown that the distribution π concentrates around $\arg \min_{x \in K} f(x)$. Thereby, we just need to prove that $\{X_k\}$ well approximates π for sufficiently large k and small η . Along with this idea, we decompose the expected risk as follows: $\mathbb{E}[N^{-1} \sum_{k=0}^{N-1} f(X_k)] - \min f = (\mathbb{E}[N^{-1} \sum_{k=0}^{N-1} f(X_k)] - \mathbb{E}_\pi f) + (\mathbb{E}_\pi f - \min f)$. Then, each term on the right hand side can be bounded in the following two lemmas.

Lemma 3.7. Under Assumptions 3.1 and 3.2, if $\beta > 0$, then it holds that

$$\mathbb{E} \left[\frac{1}{N} \sum_{k=0}^{N-1} f(X_k) \right] - \mathbb{E}_\pi f \leq C \left(\frac{1}{\lambda_* N \eta} + \frac{\sqrt{\eta} (\beta \sqrt{\eta} + (\beta \eta + d)^{3/2})}{\lambda_*} \right). \quad (6)$$

Lemma 3.8 (Lemma 15 from Lamperski (2021)). *Under Assumptions 3.1.4 and 3.2.1, we have*

$$\mathbb{E}_\pi f - \min_{x \in K} f(x) \leq \frac{d}{\beta} \log \left(2R \max \left\{ \frac{2}{r}, \frac{L\beta (r + \sqrt{r^2 + R^2})}{r \log 2} \right\} \right),$$

where L is the Lipschitz constant of f .

We can easily see that Lemma 3.6 follows after the above two lemmas. Lemma 3.8 evaluates how well the expectation of the objective with respect to π approximates the minimum value of the given function. The reader may refer to Lamperski (2021) for its proof. A similar formula of this bound was also shown by Raginsky et al. (2017) where an unconstrained problem was analyzed.

Lemma 3.7 is the key lemma for our purpose to show that the sequence generated by RGLD approximates sampling from the invariant law π given a sufficiently small step size η and a sufficiently large number of iterations N .

3.4 Strategy for Proving Lemma 3.7

Remember that the continuous-time RGLD follows the SDE given in (3). It is very involved to prove that the process (X_t) stays on K almost surely due to the reflection term. The existence and uniqueness of reflected SDEs have been studied under the name of the Skorokhod problem; see Tanaka (1979); Lions and Sznitman (1984).

In a similar way to the unconstrained setting, we can ensure the existence and uniqueness of the invariant measure of the SDE (3) (see e.g., Bubeck et al. (2018)). A concise proof is given in Appendix B for completeness.

Lemma 3.9 (Existence of Unique Invariant Measure). *Under Assumptions 3.1.3 and 3.2.1, (X_t) has a unique invariant measure π , where π is the Gibbs measure with a density defined by (4).*

Then, our purpose is reduced to showing the weak convergence of the time discretized version and bound the error for finite k and positive η . To do so, we consider the following Neumann problem associated with the Poisson equation:

$$\begin{cases} \mathcal{A}u(x) = f(x) - \mathbb{E}_\pi f, & x \in K, \\ \nabla u(x) \cdot v(x) = 0, & x \in \partial K, \end{cases} \quad (7)$$

where \mathcal{A} is the infinitesimal generator of the dynamics defined as $\mathcal{A}u(x) = \beta^{-1} \Delta u(x) - \langle \nabla f(x), \nabla u(x) \rangle$ for $x \in K$ where Δ is the Laplace operator. As is known in Miranda (1970); Freidlin (1985), the solvability of this problem requires the compatibility condition,

$$\int_K (f(x) - \mathbb{E}_\pi f) d\pi(x) = 0,$$

which holds by definition. From Assumptions 3.1.3 and 3.2.1, the Neumann problem has a unique solution (up to an additive constant) $u \in C^4(K)$ (see Miranda (1970), Gilbarg and Trudinger (1983, Chapter 6), and Lieberman (1986, Theorem 3)). Indeed, following Bencherif-Madani and Pardoux (2009, Theorem 4), we have that the solution can be written as $u(x) = \int_0^\infty \mathbb{E}[f(X_t^x) - \mathbb{E}_\pi f] dt$ where X_t^x denotes the solution of (3) at time t with the initial value x . Then, by the Ito-formula and (7), we have that

$$\frac{\partial \mathbb{E}[u(X_t^x)]}{\partial t} \Big|_{t=0} = \mathcal{A}u(x) = f(x) - \mathbb{E}_\pi f.$$

By substituting $x = X_k$, we obtain an estimate of $f(X_k) - \mathbb{E}_\pi f$ through the solution of the Poisson equation. Thus, by taking the average over $k = 0, \dots, N-1$, we have $\frac{1}{N} \sum_{k=0}^{N-1} f(X_k) - \mathbb{E}_\pi f = \frac{1}{N} \sum_{k=0}^{N-1} \partial_t \mathbb{E}[u(X_t^{X_k})] \Big|_{t=0}$, which is what we want to evaluate. Then, intuitively speaking, we approximate each term $\partial_t \mathbb{E}[u(X_t^{X_k})] \Big|_{t=0}$ on the right hand side as $\partial_t \mathbb{E}[u(X_t^{X_k})] \Big|_{t=0} \approx \eta^{-1} (\mathbb{E}[u(X_{k+1})] - \mathbb{E}[u(X_k)])$, and arrive at $\frac{1}{N} \sum_{k=0}^{N-1} f(X_k) - \mathbb{E}_\pi f \approx \frac{1}{N\eta} (\mathbb{E}[u(X_N)] - \mathbb{E}[u(X_0)])$. The right hand side of this equation can be bounded by $O(1/(\lambda_* N\eta))$ from Lemma C.1, which corresponds to the first term of the bound (6) in Lemma 3.7. The second term of the bound (6) stems from the discretization error which can be evaluated as follows.

To evaluate the discretization error, we employ a strategy that is parallel to that of Leimkuhler et al. (2020, Theorem 4.2), but we additionally require the parameter dependence of their bounds on β and d . For that purpose, we adapt the Taylor expansion of $u(X_{k+1}) - u(X_k)$ up to the third order with respect to $X_{k+1} - X_k$. Then, we bound the derivatives, which is non-trivial, by employing the *Bismut-Elworthy-Li* formula borrowed from Andres (2011); Cerrai (1998) for our Neumann problem. In that evaluation, we need to show that the derivatives of $\mathbb{E}[f(X_t^x)] - \mathbb{E}_\pi f$ with respect to x decays exponentially as t goes to infinity. We prove it by extending the argument made in the proof of Bréhier (2014, Lemma 5.4). The detailed proof of Lemma 3.7 is deferred to Appendix C. Fortunately, the reflection operation enables us to cancel the second-order derivative term and we can obtain a tighter evaluation of the discretization error.

4 Numerical Experiments

We conducted the numerical experiments to see how well RGLD performs on constrained non-convex problems in comparison with a classical algorithm, PG.

We quantified the optimization error by the gap of objective function values at the global optimal solution and the solution of the algorithms. Our focus was on how efficiently RGLD, compared with PG, finds the global optimum of a constrained non-convex problem. We also compared the performances of RGLD under different hyperparameters η , β , and dimensionalities d .

The latter half of the experiments is described in Appendix D.

4.1 Two Dimensional Problem

We start by looking at a two dimensional problem for ease of visualization. The test function is a Gaussian mixture density given by

$$f(x) = - \sum_{i=1}^M w_i \exp\left(-\frac{1}{2}(x - m_i)^\top (x - m_i)\right), \quad (8)$$

where w_i is randomly generated and m_i is a point in the meshgrid $\{-2, -1, 0, 1, 2\}^2$. The feasible region is set to the

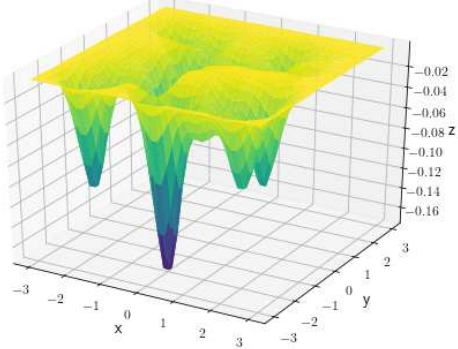


Figure 1: The objective function f in (8).

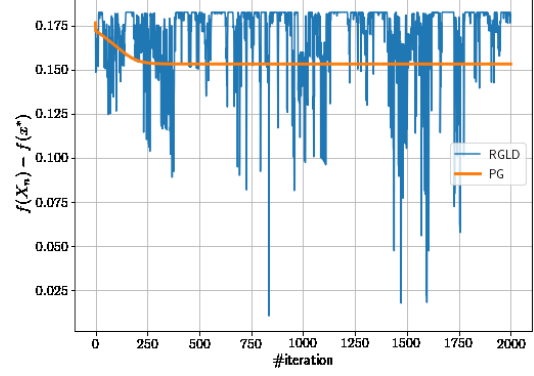


Figure 2: Convergence of the iterates by PG and RGLD. $\eta = 0.05$, $\beta = 1.0$.

region between spheres of radius 0.9 and 4 centered at the origin. Such a region is called a thick-walled sphere and appears in Chepurnenko et al. (2021); Zhang et al. (2020a). The region is non-convex and satisfies our assumptions because the boundary is smooth. Figure 1 shows a 3D plot of the objective function, which has 25 local minima. The global minimizer is at $(0, -2)$.

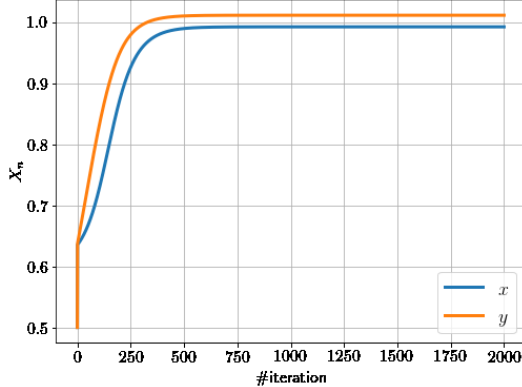
4.1.1 Comparison with PG

We found that RGLD can explore better solutions while PG becomes trapped at a local minimum. Figure 2 shows the plot of the optimization error of PG and RGLD for $\eta = 0.05$, $\beta = 1.0$ and $X_0 = (0.5, 0.5)$.

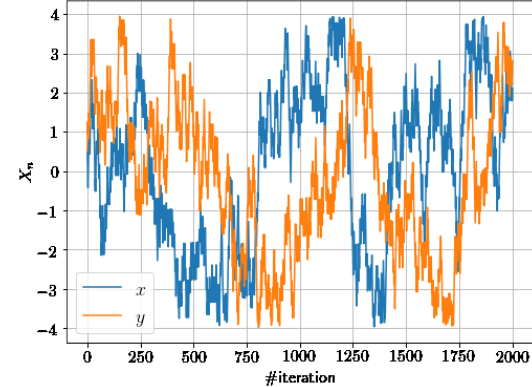
We also visualized the trajectory of each algorithm, as shown in Figure 3. We found that RGLD explores a wide range of the feasible region but seems not to converge to a global minimum at all. However, as shown in Figure 4, a larger β stabilizes the optimization, which causes RGLD to become stuck in each mode of the objective function.

4.1.2 Sensitivity to Hyperparameters

Our main theorem provides an insight on the appropriate η and β . This motivated us to examine how the values of each hyperparameter could affect the optimization. Here, we plot the cumulative minimum of the optimization error generated by the iterates of RGLD for ease of viewing. Figures 5 and 6 show the convergence of RGLD for different values of β or η . We can see that a larger β limits the solution to a narrower range of the region, resulting in slow convergence. As for η , there is a certain trade-off; that is, we need to set η large enough to search a broad range of the region within a limited number of iterates and, at the same time, the range has to be small enough to find narrow loss valleys.



PG



RGLD

Figure 3: Trajectories of the iterates by PG and RGLD.

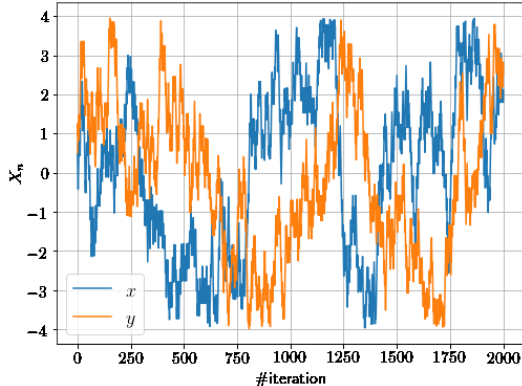
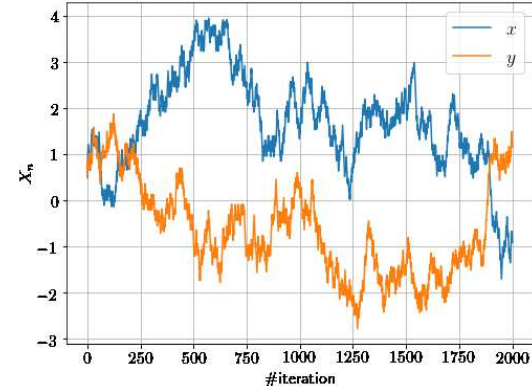

 $\beta = 1.0.$

 $\beta = 8.0.$

 Figure 4: Trajectory of RGLD with different inverse temperature parameters β .

4.1.3 Comparison of Reflection and Projection

We also compare the effects of the reflection operation and the projection operation. Figure 7 shows the convergence of the iterates generated by RGLD and PGLD. The reflection is preferable in our theoretical analysis but the result shows that these two operations make little difference in practice.

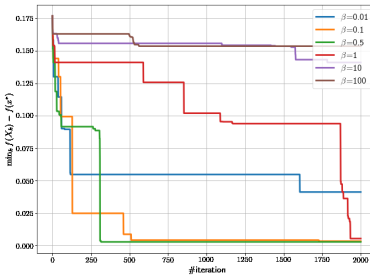
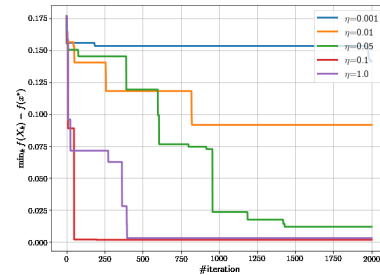
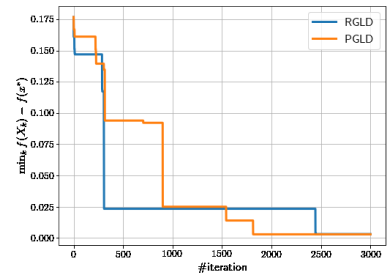

 Figure 5: RGLD under different β . $\eta = .05$.

 Figure 6: RGLD under different η . $\beta = 1.0$.


Figure 7: Comparison between RGLD and PGLD.

5 Conclusion and Future Work

We proved the sub-linear convergence rate of RGLD in solving smoothly constrained problems. Additionally, the rate faster than that of Lamperski (2021) is obtained by employing the reflection and the direct estimate of the discretization error by the Poisson equation. However, the order of λ_* is still unclear because the smallest eigenvalue problems with Neumann boundary conditions have not been studied well. Moreover, the smoothness of ∂K is essential in the analysis but not satisfied in many applications, though a smoothing operation can make a non-smooth domain have a smooth boundary.

The future works will alleviate the currently imposed assumptions towards more general unbounded non-smooth constraints. One common approach is to assume a dissipativity condition instead of the boundedness of K , as imposed in Raginsky et al. (2017); Xu et al. (2018). In this case, Barbu and Prato (2005) could be a key component with which to establish the necessary theoretical background. It is also important to extend our result to the stochastic gradient oracle version.

Acknowledgments

I would like to express my very great appreciation to our former research fellow, Michael Metel for his valuable and constructive suggestions and cooperations during the planning and development of this research. TS was partially supported by JSPS KAKENHI (18H03201), Japan Digital Design and JST CREST.

References

Andres, S. (2011). Pathwise differentiability for SDEs in a smooth domain with reflection. *Electronic Journal of Probability*, 16:845–879.

Artacho, F. J. A., Campoy, R., and Tam, M. K. (2020). The Douglas–Rachford algorithm for convex and nonconvex feasibility problems. *Mathematical Methods of Operations Research*, 91(2):201–240.

Banerjee, S. and Budhiraja, A. (2020). Parameter and dimension dependence of convergence rates to stationarity for reflecting Brownian motions. *The Annals of Applied Probability*, 30(5):2005–2029.

Barbu, V. and Prato, G. D. (2005). The Neumann problem on unbounded domains of \mathbb{R}^d and stochastic variational inequalities. *Communications in Partial Differential Equations*, 30(8):1217–1248.

Bardet, J.-B., Gozlan, N., Malrieu, F., and Zitt, P.-A. (2018). Functional inequalities for Gaussian convolutions of compactly supported measures: Explicit bounds and dimension dependence. *Bernoulli*, 24(1):333–353.

Barkhagen, M., Fleming, B., Quiles, S. G., Gondzio, J., Kalcsics, J., Kroeske, J., Sabanis, S., and Staal, A. (2019). Optimising portfolio diversification and dimensionality. *arXiv preprint arXiv:1906.00920*.

Bencherif-Madani, A. and Pardoux, É. (2009). A probabilistic formula for a Poisson equation with Neumann boundary condition. *Stochastic Analysis and Applications*, 27(4):739–746.

Bossy, M., Gobet, E., and Talay, D. (2004). A symmetrized Euler scheme for an efficient approximation of reflected diffusions. *Journal of Applied Probability*, 41(3):877–889.

Bréhier, C.-E. (2014). Approximation of the invariant measure with an Euler scheme for stochastic PDEs driven by space-time white noise. *Potential Analysis*, 40(1):1–40.

Brosse, N., Durmus, A., Moulines, É., and Pereyra, M. (2017). Sampling from a log-concave distribution with compact support with proximal Langevin Monte Carlo. In Kale, S. and Shamir, O., editors, *Proceedings of the 2017 Conference on Learning Theory*, volume 65 of *Proceedings of Machine Learning Research*, pages 319–342. PMLR.

Bubeck, S., Eldan, R., and Lehec, J. (2018). Sampling from a log-concave distribution with projected Langevin Monte Carlo. *Discrete & Computational Geometry*, 59(4):757–783.

Cattiaux, P., León, J. R., and Prieur, C. (2017). Invariant density estimation for a reflected diffusion using an Euler scheme. *Monte Carlo Methods and Applications*, 23(2):71–88.

Cerrai, S. (1998). Some results for second order elliptic operators having unbounded coefficients. *Differential and Integral Equations*, 11(4):561–588.

Chen, P., Lu, J., and Xu, L. (2021). Approximation to stochastic variance reduced gradient Langevin dynamics by stochastic delay differential equations. *arXiv preprint arXiv:2106.04357*.

Chen, X. and Lou, Y. (2012). Effects of diffusion and advection on the smallest eigenvalue of an elliptic operator and their applications. *Indiana University Mathematics Journal*, 61(1):45–80.

Chepurnenko, A., Litvinov, S., Meskhi, B., and Beskopylny, A. (2021). Optimization of thick-walled viscoelastic hollow polymer cylinders by artificial heterogeneity creation: Theoretical aspects. *Polymers*, 13(15).

Chiang, T.-S., Hwang, C.-R., and Sheu, S. J. (1987). Diffusion for global optimization in \mathbb{R}^n . *SIAM Journal on Control and Optimization*, 25(3):737–753.

Dalalyan, A. (2017). Further and stronger analogy between sampling and optimization: Langevin Monte Carlo and gradient descent. In Kale, S. and Shamir, O., editors, *Proceedings of the 2017 Conference on Learning Theory*, volume 65 of *Proceedings of Machine Learning Research*, pages 678–689. PMLR.

Ding, D. and Zhang, Y.-y. (2008). Numerical solutions for reflected stochastic differential equations.

Dupuis, P. and Ramanan, K. (1999). Convex duality and the Skorokhod problem. I. *Probability Theory and Related Fields*, 115(2):153–195.

Durmus, A., Moulines, E., and Pereyra, M. (2018). Efficient Bayesian computation by proximal Markov chain Monte Carlo: when Langevin meets Moreau. *SIAM Journal on Imaging Sciences*, 11(1):473–506.

Freidlin, M. I. (1985). *Functional Integration and Partial Differential Equations*, volume 109. Princeton University Press.

Garroni, M. G. and Menaldi, J. L. (1992). *Green Functions for Second Order Parabolic Integro-Differential Problems*, volume 275. Chapman and Hall/CRC.

Gayrard, V., Bovier, A., and Klein, M. (2005). Metastability in reversible diffusion processes II: Precise asymptotics for small eigenvalues. *Journal of the European Mathematical Society*, 7(1):69–99.

Gelfand, S. B. and Mitter, S. K. (1991). Recursive stochastic algorithms for global optimization in \mathbb{R}^d . *SIAM Journal on Control and Optimization*, 29(5):999–1018.

Geman, S. and Hwang, C.-R. (1986). Diffusions for global optimization. *SIAM Journal on Control and Optimization*, 24(5):1031–1043.

Gilbarg, D. and Trudinger, N. S. (1983). *Elliptic Partial Differential Equations of Second Order*. Springer.

Hinder, O. and Ye, Y. (2018). Worst-case iteration bounds for log barrier methods for problems with nonconvex constraints. *arXiv preprint arXiv:1807.00404*.

Hsieh, Y.-P., Kavis, A., Rolland, P., and Cevher, V. (2018). Mirrored Langevin dynamics. In Bengio, S., Wallach, H., Larochelle, H., Grauman, K., Cesa-Bianchi, N., and Garnett, R., editors, *Advances in Neural Information Processing Systems*, volume 31, pages 2878–2887. Curran Associates, Inc.

Kingma, D. P. and Ba, J. (2014). Adam: a method for stochastic optimization. *arXiv preprint arXiv:1412.6980*.

Lamperski, A. (2021). Projected stochastic gradient Langevin algorithms for constrained sampling and non-convex learning. In Belkin, M. and Kpotufe, S., editors, *Proceedings of Thirty Fourth Conference on Learning Theory*, volume 134 of *Proceedings of Machine Learning Research*, pages 2891–2937. PMLR.

Leimkuhler, B., Sharma, A., and Tretyakov, M. V. (2020). Simplest random walk for approximating Robin boundary value problems and ergodic limits of reflected diffusions. *arXiv preprint arXiv:2006.15670*.

Li, H. and Lin, Z. (2015). Accelerated proximal gradient methods for nonconvex programming. In Cortes, C., Lawrence, N., Lee, D., Sugiyama, M., and Garnett, R., editors, *Advances in Neural Information Processing Systems*, volume 28, pages 379–387. Curran Associates, Inc.

Lieberman, G. M. (1986). Intermediate Schauder estimates for oblique derivative problems. *Archive for Rational Mechanics and Analysis*, 93(2):129–134.

Lin, Q., Ma, R., and Xu, Y. (2019). Inexact proximal-point penalty methods for constrained non-convex optimization. *arXiv preprint arXiv:1908.11518*.

Lions, P.-L. and Sznitman, A.-S. (1984). Stochastic differential equations with reflecting boundary conditions. *Communications on Pure and Applied Mathematics*, 37(4):511–537.

Masnadi-shirazi, H. and Vasconcelos, N. (2009). On the design of loss functions for classification: theory, robustness to outliers, and savageboost. In Koller, D., Schuurmans, D., Bengio, Y., and Bottou, L., editors, *Advances in Neural Information Processing Systems*, volume 21, pages 1049–1056. Curran Associates, Inc.

Miranda, C. (1970). *Partial Differential Equations of Elliptic Type*, volume 2. Springer.

Parpas, P., Rustem, B., and Pistikopoulos, E. N. (2006). Linearly constrained global optimization and stochastic differential equations. *Journal of Global Optimization*, 36(2):191–217.

Patterson, S. and Teh, Y. W. (2013). Stochastic gradient Riemannian Langevin dynamics on the probability simplex. In Burges, C. J. C., Bottou, L., Welling, M., Ghahramani, Z., and Weinberger, K. Q., editors, *Advances in Neural Information Processing Systems*, volume 26, pages 3102–3110. Curran Associates, Inc.

Peng, R., Zhang, G., and Zhou, M. (2019). Asymptotic behavior of the principal eigenvalue of a linear second order elliptic operator with small/large diffusion coefficient. *SIAM Journal on Mathematical Analysis*, 51(6):4724–4753.

Pereyra, M. (2016). Proximal Markov chain Monte Carlo algorithms. *Statistics and Computing*, 26(4):745–760.

Raginsky, M., Rakhlin, A., and Telgarsky, M. (2017). Non-convex learning via stochastic gradient Langevin dynamics: a nonasymptotic analysis. In *Proceedings of the 2017 Conference on Learning Theory*, volume 65 of *Proceedings of Machine Learning Research*, pages 1674–1703.

Salim, A., Kovalev, D., and Richtárik, P. (2019). Stochastic proximal Langevin algorithm: Potential splitting and nonasymptotic rates. In Wallach, H., Larochelle, H., Beygelzimer, A., d’Alché-Buc, F., Fox, E., and Garnett, R., editors, *Advances in Neural Information Processing Systems*, volume 32, pages 6653–6664. Curran Associates, Inc.

Salim, A. and Richtarik, P. (2020). Primal dual interpretation of the proximal stochastic gradient Langevin algorithm. In Larochelle, H., Ranzato, M., Hadsell, R., Balcan, M. F., and Lin, H., editors, *Advances in Neural Information Processing Systems*, volume 33, pages 3786–3796. Curran Associates, Inc.

Signoretto, M., De Lathauwer, L., and Suykens, J. A. K. (2013). Learning tensors in reproducing kernel Hilbert spaces with multilinear spectral penalties. *arXiv preprint arXiv:1310:4977*.

Suzuki, T., Kanagawa, H., Kobayashi, H., Shimizu, N., and Tagami, Y. (2016). Minimax optimal alternating minimization for kernel nonparametric tensor learning. In Lee, D., Sugiyama, M., Luxburg, U., Guyon, I., and Garnett, R., editors, *Advances in Neural Information Processing Systems*, volume 29, pages 3783–3791. Curran Associates, Inc.

Tanaka, H. (1979). Stochastic differential equations with reflecting boundary condition in convex regions. *Hiroshima Mathematical Journal*, 9(1):163–177.

Vempala, S. and Wibisono, A. (2019). Rapid convergence of the unadjusted Langevin algorithm: Isoperimetry suffices. In Wallach, H., Larochelle, H., Beygelzimer, A., d’Alché-Buc, F., Fox, E., and Garnett, R., editors, *Advances in Neural Information Processing Systems*, volume 32, pages 8094–8106. Curran Associates, Inc.

Wang, X., Lei, Q., and Panageas, I. (2020). Fast convergence of Langevin dynamics on manifold: Geodesics meet log-Sobolev. In Larochelle, H., Ranzato, M., Hadsell, R., Balcan, M. F., and Lin, H., editors, *Advances in Neural Information Processing Systems*, volume 33, pages 18894–18904. Curran Associates, Inc.

Welling, M. and Teh, Y. W. (2011). Bayesian learning via stochastic gradient Langevin dynamics. In *Proceedings of the 28th International Conference on Machine Learning*, pages 681–688.

Wen, F., Chu, L., Liu, P., and Qiu, R. C. (2018). A survey on nonconvex regularization-based sparse and low-rank recovery in signal processing, statistics, and machine learning. *IEEE Access*, 6:69883–69906.

Xie, Y. and Wright, S. J. (2021). Complexity of proximal augmented Lagrangian for nonconvex optimization with nonlinear equality constraints. *Journal of Scientific Computing*, 86(3):1–30.

Xu, P., Chen, J., Zou, D., and Gu, Q. (2018). Global convergence of Langevin dynamics based algorithms for non-convex optimization. In Bengio, S., Wallach, H., Larochelle, H., Grauman, K., Cesa-Bianchi, N., and Garnett, R., editors, *Advances in Neural Information Processing Systems*, volume 31, pages 3122–3133. Curran Associates, Inc.

Zhang, J., Oueslati, A., Shen, W., De Saxcé, G., Nguyen, A. D., Zhu, Q., and Shao, J. (2020a). Shakedown analysis of a hollow sphere by interior-point method with non-linear optimization. *International Journal of Mechanical Sciences*, 175:105515.

Zhang, K. S., Peyré, G., Fadili, J., and Pereyra, M. (2020b). Wasserstein control of mirror Langevin Monte Carlo. In Abernethy, J. and Agarwal, S., editors, *Proceedings of Thirty Third Conference on Learning Theory*, volume 125 of *Proceedings of Machine Learning Research*, pages 3814–3841. PMLR.

Zhang, X., Wang, L., and Gu, Q. (2018). A unified framework for nonconvex low-rank plus sparse matrix recovery. In Storkey, A. and Perez-Cruz, F., editors, *Proceedings of the Twenty-First International Conference on Artificial Intelligence and Statistics*, volume 84 of *Proceedings of Machine Learning Research*, pages 1097–1107. PMLR.

Zhang, Y., Liang, P., and Charikar, M. (2017). A hitting time analysis of stochastic gradient Langevin dynamics. In *Proceedings of the 2017 Conference on Learning Theory*, volume 65 of *Proceedings of Machine Learning Research*, pages 1980–2022.

Zou, D., Xu, P., and Gu, Q. (2021). Faster convergence of stochastic gradient Langevin dynamics for non-log-concave sampling. In de Campos, C. and Maathuis, M. H., editors, *Proceedings of the Thirty-Seventh Conference on Uncertainty in Artificial Intelligence*, volume 161 of *Proceedings of Machine Learning Research*, pages 1152–1162. PMLR.

A Proof of Theorem 3.4

First, it is obvious that

$$\min_{k \in [N]} f(X_k) \leq \frac{1}{N} \sum_{k=0}^{N-1} f(X_k), \quad \mathbb{E} \left[\min_{k \in [N]} f(X_k) \right] - \min f \leq \mathbb{E} \left[\frac{1}{N} \sum_{k=0}^{N-1} f(X_k) \right] - \min f.$$

Thus, it suffices to show

$$\mathbb{E} \left[\frac{1}{N} \sum_{k=0}^{N-1} f(X_k) \right] - \min f \preceq \epsilon + \frac{d}{\beta} \log \beta$$

to conclude that $\mathbb{E} [\min_{k \in [N]} f(X_k)] - \min f \leq \epsilon + d\beta^{-1} \log \beta$. From Lemma 3.6, it is enough to establish

$$\frac{1}{\lambda_* N \eta} + \frac{\sqrt{\eta} (\beta \sqrt{\eta} + (\beta \eta + d)^{3/2})}{\lambda_*} \preceq \epsilon.$$

From the condition on η , we have $\lambda_*^{-1} \beta \eta \preceq \epsilon$, $\lambda_*^{-1} (d\eta)^{3/2} \preceq \epsilon$. Moreover, we have $\lambda_*^{-1} \beta^{3/2} \eta^2 \preceq \lambda_* \epsilon^2 / \sqrt{\beta}$ and, noticing that $\lambda_*, \epsilon, \beta^{-1/2} \preceq 1$, we have $\lambda_* \epsilon^2 / \sqrt{\beta} \preceq \epsilon$. Finally, from the condition on N , we have $(\lambda_* N \eta)^{-1} \preceq \epsilon$.

The theorem follows by combining all the above.

B Proof of Lemma 3.9

From Assumptions 3.1.3 and 3.2.1, there exists a unique invariant measure of (X_t) . Thus, it suffices to show that π is stationary. It holds if and only if

$$\int_K \mathcal{A} u d\pi = 0 \quad \forall u \in \text{dom} \mathcal{A},$$

where \mathcal{A} is the infinitesimal generator of (X_t) . The infinitesimal generator \mathcal{A} is represented by

$$\mathcal{A} u(x) = \frac{1}{\beta} \Delta u(x) - \nabla f(x) \cdot \nabla u(x) \quad x \in K,$$

where Δ is the Laplace operator, and the domain of \mathcal{A} is

$$\text{dom} \mathcal{A} = \{u \mid \nabla u(x) \cdot v(x) = 0, \quad x \in \partial K\}.$$

Then, one can derive

$$\begin{aligned} \int_K \mathcal{A} u d\pi &= \int_K \left(\frac{1}{\beta} \Delta u(x) - \nabla f(x) \cdot \nabla u(x) \right) \frac{\exp(-\beta f(x))}{\int_K \exp(-\beta f(y)) dy} dx \\ &= \int_K \nabla \cdot \left(\frac{\exp(-\beta f(x)) \nabla u(x)}{\beta \int_K \exp(-\beta f(y)) dy} \right) dx \\ &= \frac{1}{\beta \int_K \exp(-\beta f(y)) dy} \int_{\partial K} \exp(-\beta f(x)) \nabla u(x) \cdot v(x) dx = 0, \end{aligned}$$

from the definition of π and \mathcal{A} , the divergence theorem, and the condition of u .

C Proof of Lemma 3.7

C.1 Error Analysis via Taylor Expansion

In this part, we aim to establish a relationship between the Taylor expansion of the solution u of (7) and the error analysis of the invariant measure approximation. First, from Garroni and Menaldi (1992, Proposition 1.17), it is known that $u \in C^4(K)$ can be extended to a function in $C^4(K \cup K_{-r'})$, where r' is the supremum of positive numbers such that the reflection of any $x \in K_{-r'}$ is well-defined. This implies that u and its derivatives up to fourth order are uniformly bounded on $K \cup K_{-r'}$. We often identify the i -th derivative of u with a multilinear operator on \mathbb{R}^d , $D^i u$, by using the Riesz representation theorem. For example, we identify $\Delta u(x)$ at $x \in K \cup K_{-r'}$ with the bilinear

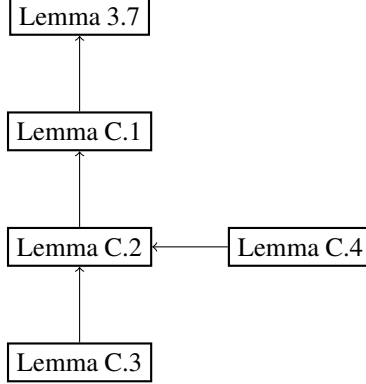


Figure 8: Relations between Statements Used to Prove Lemma 3.7

operator $D^2u(x) : \mathbb{R}^d \times \mathbb{R}^d \rightarrow \mathbb{R}$. We write applying the operator to $y, z \in \mathbb{R}^d$ as $D^2u(x)(y, z)$. We also define the operator norm of $D^i u(x)$ by

$$\|D^i u(x)\| = \sup \frac{D^i u(x)(x_1, \dots, x_i)}{\prod_{j=1}^i \|x_j\|}.$$

For simplicity, we let $\|D^i u\| = \sup_{x \in K \cup K_{-r'}} \|D^i u(x)\|$. Analogically, we let $D^0 f$ to be f itself and $\|D^0 f\|$ to be sup norm of f , $\|f\|_\infty$.

Then, we discuss the Taylor expansion of $u(X_{k+1})$ of (7) around X_k . Following Leimkuhler et al. (2020), we write $u_k := u(X_k)$, $u'_k := u(X'_k)$, $v_k^\pi := v(X_k^\pi)$ and $f_k := f(X_k)$, where X'_k is introduced in Algorithm 2.1 and $X_k^\pi := \mathcal{P}_K(X'_k)$. Following this notation, we write

$$u_{k+1} - u_k = (u_{k+1} - u'_{k+1}) + (u'_{k+1} - u_k).$$

For the first term, since X_{k+1}^π is the midpoint between X'_{k+1} and X_{k+1} by (2), we can write

$$\begin{aligned} X_{k+1} &= \mathcal{R}_K(X'_{k+1}) = X'_{k+1} - 2r_{k+1}v_{k+1}^\pi = X_{k+1}^\pi - r_{k+1}v_{k+1}^\pi, \\ X'_{k+1} &= X_{k+1}^\pi - r_{k+1}v_{k+1}^\pi + r_{k+1}v_{k+1}^\pi = X_{k+1}^\pi + r_{k+1}v_{k+1}^\pi, \end{aligned}$$

where $r_k = \|X_k^\pi - X_k\|$. Then, we obtain

$$u_{k+1} - u'_{k+1} = u(X_{k+1}^\pi - r_{k+1}v_{k+1}^\pi) - u(X_{k+1}^\pi + r_{k+1}v_{k+1}^\pi).$$

Using a Taylor expansion up to third order, we obtain

$$\begin{aligned} &u(X_{k+1}^\pi - r_{k+1}v_{k+1}^\pi) - u(X_{k+1}^\pi + r_{k+1}v_{k+1}^\pi) \\ &= \left(u_{k+1}^\pi - r_{k+1}Du_{k+1}^\pi(v_{k+1}^\pi) + \frac{r_{k+1}^2}{2}D^2u_{k+1}^\pi(v_{k+1}^\pi, v_{k+1}^\pi) \right. \\ &\quad \left. - \frac{r_{k+1}^3}{6}D^3u(X_{k+1}^\pi - \alpha_1 r_{k+1}v_{k+1}^\pi)(v_{k+1}^\pi, v_{k+1}^\pi, v_{k+1}^\pi) \right) \\ &\quad - \left(u_{k+1}^\pi + r_{k+1}Du_{k+1}^\pi(v_{k+1}^\pi) + \frac{r_{k+1}^2}{2}D^2u_{k+1}^\pi(v_{k+1}^\pi, v_{k+1}^\pi) \right. \\ &\quad \left. + \frac{r_{k+1}^3}{6}D^3u(X_{k+1}^\pi + \alpha_2 r_{k+1}v_{k+1}^\pi)(v_{k+1}^\pi, v_{k+1}^\pi, v_{k+1}^\pi) \right), \end{aligned} \tag{9}$$

where $\alpha_1, \alpha_2 \in [0, 1]$ are constants. Here, we have used the mean value theorem in the third derivative term. The second derivative term is canceled out and thus we have

$$\begin{aligned} u_{k+1} - u'_{k+1} &= -\frac{r_{k+1}^3}{6}D^3u(X_{k+1}^\pi - \alpha_1 r_{k+1}v_{k+1}^\pi)(v_{k+1}^\pi, v_{k+1}^\pi, v_{k+1}^\pi) \\ &\quad - \frac{r_{k+1}^3}{6}D^3u(X_{k+1}^\pi + \alpha_2 r_{k+1}v_{k+1}^\pi)(v_{k+1}^\pi, v_{k+1}^\pi, v_{k+1}^\pi) \\ &\geq -\frac{r_{k+1}^3}{3}\|D^3u\|, \end{aligned} \tag{10}$$

since $Du_{k+1}^\pi(v_{k+1}^\pi) = \nabla u(X_{k+1}^\pi) \cdot v_{k+1}^\pi = 0$ from (7). The last inequality comes from the definition of the operator norm and $\|v_{k+1}^\pi\| \in \{0, 1\}$.

In the same way, we obtain

$$\begin{aligned}
 u'_{k+1} - u_k &= u \left(X_k - \eta \nabla f_k + \sqrt{\frac{2\eta}{\beta}} \xi_{k+1} \right) - u_k \\
 &= Du_k \left(-\eta \nabla f_k + \sqrt{\frac{2\eta}{\beta}} \xi_{k+1} \right) \\
 &\quad + \frac{1}{2} D^2 u_k \left(-\eta \nabla f_k + \sqrt{\frac{2\eta}{\beta}} \xi_{k+1}, -\eta \nabla f_k + \sqrt{\frac{2\eta}{\beta}} \xi_{k+1} \right) \\
 &\quad + \frac{1}{6} D^3 u \left(X_k + \alpha_3 \left(-\eta \nabla f_k + \sqrt{\frac{2\eta}{\beta}} \xi_{k+1} \right) \right) \left(-\eta \nabla f_k + \sqrt{\frac{2\eta}{\beta}} \xi_{k+1}, \right. \\
 &\quad \left. -\eta \nabla f_k + \sqrt{\frac{2\eta}{\beta}} \xi_{k+1}, -\eta \nabla f_k + \sqrt{\frac{2\eta}{\beta}} \xi_{k+1} \right),
 \end{aligned} \tag{11}$$

where $\alpha_3 \in [0, 1]$ is some constant. Since $\mathbb{E}[\xi_{k+1}] = 0$, taking the expectation yields

$$\begin{aligned}
 \mathbb{E}[u'_{k+1} - u_k] &= \mathbb{E} \left[-\eta \nabla f_k \dot{\nabla} u_k + \frac{\eta}{\beta} \Delta u_k + \frac{\eta^2}{2} D^2 u_k (\nabla f_k, \nabla f_k) \right. \\
 &\quad \left. + \frac{1}{6} D^3 u \left(X_k + \alpha_3 \left(-\eta \nabla f_k + \sqrt{\frac{2\eta}{\beta}} \xi_{k+1} \right) \right) \left(-\eta \nabla f_k + \sqrt{\frac{2\eta}{\beta}} \xi_{k+1}, \right. \right. \\
 &\quad \left. \left. -\eta \nabla f_k + \sqrt{\frac{2\eta}{\beta}} \xi_{k+1}, -\eta \nabla f_k + \sqrt{\frac{2\eta}{\beta}} \xi_{k+1} \right) \right].
 \end{aligned} \tag{12}$$

Then, by the definition of \mathcal{A} , we obtain

$$\begin{aligned}
 \mathbb{E}[u'_{k+1} - u_k] &= \mathbb{E} \left[\eta \mathcal{A} u_k + \frac{\eta^2}{2} D^2 u_k (\nabla f_k, \nabla f_k) \right. \\
 &\quad \left. + \frac{1}{6} D^3 u \left(X_k + \alpha_3 \left(-\eta \nabla f_k + \sqrt{\frac{2\eta}{\beta}} \xi_{k+1} \right) \right) \left(-\eta \nabla f_k + \sqrt{\frac{2\eta}{\beta}} \xi_{k+1}, \right. \right. \\
 &\quad \left. \left. -\eta \nabla f_k + \sqrt{\frac{2\eta}{\beta}} \xi_{k+1}, -\eta \nabla f_k + \sqrt{\frac{2\eta}{\beta}} \xi_{k+1} \right) \right] \\
 &= \mathbb{E} \left[\eta (f_k - \mathbb{E}_\pi f) + \frac{\eta^2}{2} D^2 u(X_k) (\nabla f_k, \nabla f_k) \right. \\
 &\quad \left. + \frac{1}{6} D^3 u \left(X_k + \alpha_3 \left(-\eta \nabla f_k + \sqrt{\frac{2\eta}{\beta}} \xi_{k+1} \right) \right) \left(-\eta \nabla f_k + \sqrt{\frac{2\eta}{\beta}} \xi_{k+1}, \right. \right. \\
 &\quad \left. \left. -\eta \nabla f_k + \sqrt{\frac{2\eta}{\beta}} \xi_{k+1}, -\eta \nabla f_k + \sqrt{\frac{2\eta}{\beta}} \xi_{k+1} \right) \right],
 \end{aligned} \tag{13}$$

We apply (10), (13) to

$$\mathbb{E}[u'_{k+1} - u_k] = \mathbb{E}[u_{k+1} - u_k] - \mathbb{E}[u_{k+1} - u'_{k+1}],$$

to obtain

$$\begin{aligned}
 \mathbb{E} \left[\eta (f_k - \mathbb{E}_\pi f) + \frac{\eta^2}{2} D^2 u(X_k) (\nabla f_k, \nabla f_k) \right. \\
 &\quad \left. + \frac{1}{6} D^3 u \left(X_k + \alpha_3 \left(-\eta \nabla f_k + \sqrt{\frac{2\eta}{\beta}} \xi_{k+1} \right) \right) \left(-\eta \nabla f_k + \sqrt{\frac{2\eta}{\beta}} \xi_{k+1}, \right. \right. \\
 &\quad \left. \left. -\eta \nabla f_k + \sqrt{\frac{2\eta}{\beta}} \xi_{k+1}, -\eta \nabla f_k + \sqrt{\frac{2\eta}{\beta}} \xi_{k+1} \right) \right] \\
 &\leq \mathbb{E}[u_{k+1} - u_k] + \frac{r_{k+1}^3}{3} \|D^3 u\|.
 \end{aligned}$$

Since $\|\xi_{k+1}\| = \sqrt{d}$, and $\|\nabla f(X_k)\|$ is uniformly bounded, we have

$$\mathbb{E}[\eta(f_k - \mathbb{E}_\pi f)] \leq \mathbb{E}[u_{k+1} - u_k] + \frac{r_{k+1}^3}{3} \|D^3 u\| + C\eta^2 \|D^2 u\| + C\|D^3 u\| \left(\eta + \sqrt{\frac{d\eta}{\beta}}\right)^3. \quad (14)$$

To obtain the upper bounds of the right-hand side, we will use the following lemma, which is proved in Appendix C.2.

Lemma C.1. *There exists a constant $C_f > 0$ depending only on $\|D^i f\|$ ($i = 0, 2, 3$) such that, for any $\beta > 0$,*

$$\forall x \in K \cup K_{-r'}, \quad \|D^i u(x)\| < \frac{C_f \beta^{i/2}}{\lambda_*} \quad (i = 0, 1, 2, 3),$$

where r' is the supremum of positive numbers such that the reflection of any $x \in K_{-r'}$ is well-defined.

Completing the Proof of Lemma 3.7 Therefore, combining (14) with Lemma C.1 yields the following inequality:

$$\mathbb{E}[\eta(f(X_k) - \mathbb{E}_\pi f)] < \mathbb{E}[u(X_{k+1}) - u(X_k)] + \frac{C}{\lambda_*} \left(\beta^{3/2} r_{k+1}^3 + \beta\eta^2 + \beta^{3/2}\eta^3 + (d\eta)^{3/2}\right).$$

Since $r_{k+1} = O(\eta + \sqrt{d\eta/\beta})$, we obtain

$$\mathbb{E}[\eta(f(X_k) - \mathbb{E}_\pi f)] < \mathbb{E}[u(X_{k+1}) - u(X_k)] + \frac{C\eta^{3/2}(\beta\sqrt{\eta} + (\beta\eta + d)^{3/2})}{\lambda_*}.$$

Thus,

$$\begin{aligned} \frac{1}{N} \sum_{k=1}^N \mathbb{E}[f(X_k) - \mathbb{E}_\pi f] &< \mathbb{E}\left[\frac{u(X_N) - u(X_0)}{N\eta}\right] + \frac{C\sqrt{\eta}(\beta\sqrt{\eta} + (\beta\eta + d)^{3/2})}{\lambda_*} \\ &< \frac{C}{\lambda_* N\eta} + \frac{C\sqrt{\eta}(\beta\sqrt{\eta} + (\beta\eta + d)^{3/2})}{\lambda_*}, \end{aligned}$$

by Lemma C.1 again.

C.2 Proof of Lemma C.1

In this subsection, we prove Lemma C.1. From Bencherif-Madani and Pardoux (2009, Theorem 4), we have the following probabilistic representation of u :

$$u(x) = \int_0^\infty \mathbb{E}[f(X_t^x) - \mathbb{E}_\pi f] dt,$$

where X_t^x denotes the solution of (3) at time t starting from x . Let $\phi(t, x) := \mathbb{E}[f(X_t^x) - \mathbb{E}_\pi f]$; we will prove the following.

Lemma C.2. *There exists a constant $C > 0$ with the same constant as in Lemma C.1 such that, for any $\beta > 0$, $t \geq 0$, and $x \in K$,*

$$\|D^i \phi(t, x)\| < C\beta^{i/2} e^{-\lambda_* t} \quad (i = 1, 2, 3),$$

where λ_* is the spectral gap defined in (5).

Integrating over t completes the proof. Thus, it suffices to show Lemma C.2. First, we state the following lemma using the Bismut-Elworthy-Li formula.

Lemma C.3 (Cerrai (1998, Propositions 6.1, 6.3, 6.4)). *For any $g(x) \in C^4(K \cup K_{-r'})$, there exists a constant $C > 0$ such that for any $\beta > 0$, $0 < t \leq 1$, and $x \in K \cup K_{-r'}$,*

$$\|D^i \Phi(t, x)\| < C \left(\frac{\beta}{t}\right)^{i/2} \|g\|_\infty, \quad (i = 1, 2, 3),$$

where $\Phi(t, x) = \mathbb{E}[g(X_t^x)]$. C depends polynomially on the exponential of the supremum of $\|D^2 f\|$, $\|D^3 f\|$, $\|D^4 f\|$.

Proof. Most of the proof is given in Cerrai (1998). The statement is rectified by noticing that $N = \sqrt{\beta/2}$. \square

Then, the convergence rate of ϕ is represented by the spectral gap λ_* .

Lemma C.4. (Freidlin, 1985, Chapter II) *There exists a constant C such that for any $t \geq 0$,*

$$|\phi(t, x)| < C e^{-\lambda_* t},$$

where λ_* is the spectral gap defined in (5).

Let us see that we can prove Lemma C.2 from Lemmas C.3 and C.4. We define

$$S := \{t \geq 0 \mid X_t(x) \in \partial K\}, \quad r(t) := \sup(S \cap [0, t]),$$

where $x \in K$. As preparation, we define three equations and their solutions. For $h \in \mathbb{R}^d$ and $t \geq 0$, let $Y_t^h(x)$ be the solution of the derivative equation,

$$\begin{cases} Y_t^h = h - \int_0^t \Delta f(X_s^x) Y_s^h ds, & \text{if } t < \inf S, \\ Y_t^h = \mathcal{P}_{X_{r(t)}^x}(Y_{r(t)-}^h) - \int_{r(t)}^t \Delta f(X_s^x) Y_s^h ds, & \text{if } t \geq \inf S, \end{cases}$$

where \mathcal{P}_x is defined by

$$\mathcal{P}_x(z) = z - \langle z, v(x) \rangle v(x), \quad \forall x \in \partial K, z \in \mathbb{R}^d,$$

and $Y_{r(t)-}^h$ is the left-hand limit of Y_t^h as $t \uparrow r(t)$. It is possible to show (see Andres (2011)) that $Y_t^h(x)$ is the first-order derivative in probability of X_t^x with respect to x along the direction $h \in \mathbb{R}^d$. We let $Z_t^{h,k}(x)$ be the solution of the problem,

$$\begin{cases} Z_t^{h,k} = - \int_0^t \Delta f(X_s^x) Z_s^{h,k} + D^3 f(X_s^x)(Y_s^h, Y_s^k) ds, & \text{if } t < \inf S, \\ Z_t^{h,k} = - \int_{r(t)}^t \Delta f(X_s^x) Z_s^{h,k} + D^3 f(X_s^x)(Y_s^h, Y_s^k) ds, & \text{if } t \geq \inf S. \end{cases}$$

As with the first derivative, it is possible to show (see Cerrai (1998)) that $Z_t^{h,k}(x)$ is the second-order derivative in probability of X_t^x with respect to x along the directions h and k . Finally, let $V_t^{l,m,n}(x)$ be the solution of the following equation:

$$\begin{cases} V_t^{l,m,n} = - \int_0^t \Delta f(X_s^x) V_s^{l,m,n} + D^4 f(X_s^x)(Y_s^l, Y_s^m, Y_s^n) \\ \quad + \frac{1}{2} \sum_{\sigma \in S_3} D^3 f(X_s^x)(Y_s^{\sigma(l)}, Z_s^{\sigma(m), \sigma(n)}) ds, & \text{if } t < \inf S, \\ V_t^{l,m,n} = - \int_{r(t)}^t \Delta f(X_s^x) V_s^{l,m,n} + D^4 f(X_s^x)(Y_s^l, Y_s^m, Y_s^n) \\ \quad + \frac{1}{2} \sum_{\sigma \in S_3} D^3 f(X_s^x)(Y_s^{\sigma(l)}, Z_s^{\sigma(m), \sigma(n)}) ds, & \text{if } t \geq \inf S, \end{cases}$$

where S_3 denotes the set of all permutations of three elements. As with the first two derivatives, $V_t^{l,m,n}(x)$ is the third-order derivative in probability of X_t^x with respect to x along the directions l, m and n .

Proof of Lemma C.2. In the case of $t_0 \geq 1$, applying Lemma C.3 to $t := 1$, $g(x) := \phi(t_0 - 1, x)$ and evaluating $\|g\|_\infty$ by Lemma C.4 yield

$$\|D^i \mathbb{E}[\phi(t_0 - 1, X_1^x)]\| < C \beta^{i/2} e^{-\lambda_*(t_0 - 1)} \Leftrightarrow \|D^i \phi(t_0, x)\| < C \beta^{i/2} e^{-\lambda_*(t_0 - 1)} < C \beta^{i/2} e^{-\lambda_* t_0}.$$

Replacing t_0 with t proves the statement. Otherwise, we start by proving that Y_t , Z_t and V_t are bounded for any $0 < t \leq 1$.

$$\begin{aligned} \|Y_t^h\| &\leq \|h\| + \int_0^t \|\Delta f(X_s^x) Y_s^h\| ds \\ &\leq \|h\| + C \int_0^t \|Y_s^h\| ds, \quad \text{if } t < \inf S. \end{aligned}$$

Then, from Gronwall's inequality,

$$\|Y_t^h\| \leq \|h\| \exp\left(\int_0^t C ds\right) \leq \|h\| \exp\left(\int_0^1 C ds\right) \leq \|h\| e^C < C\|h\|.$$

If $t \geq \inf S$, by making a recursion argument, we have

$$\|Y_t^h\| < C \left\| \mathcal{P}_{X_{r(t)}^x} (Y_{r(t)-}^h) \right\| < C \left\| Y_{r(t)-}^h \right\| < C\|h\|.$$

As for Z_t , from the result on Y_t^h , we have

$$\|Z_t^{h,k}\| \leq \int_0^t C \|Z_s^{h,k}\| + C\|h\|\|k\| ds \leq C\|h\|\|k\| + \int_0^t C \|Z_s^{h,k}\| ds.$$

Moreover, from Gronwall's inequality, we get $\|Z_t^{h,k}\| \leq C\|h\|\|k\|$. By the same argument, it follows that $V_t^{l,m,n} \leq C\|l\|\|m\|\|n\|$. By the way, $D^i\phi(t, x)$ ($i = 1, 2, 3$) can be calculated in the following way:

$$\begin{aligned} D\phi(t, x) \cdot h &= \mathbb{E} [Df(X_t^x) \cdot Y_t^h(x)], \\ D^2\phi(t, x) (h, k) &= \mathbb{E} [D^2f(X_t^x) (Y_t^h, Y_t^k) + Df(X_t^x) \cdot Z_t^{h,k}], \\ D^3\phi(t, x) (l, m, n) &= \mathbb{E} [D^3f(X_t^x) (Y_t^l, Y_t^m, Y_t^n) + Df(X_t^x) \cdot V_t^{l,m,n}] \\ &\quad + \mathbb{E} \left[\frac{1}{2} \sum_{\sigma \in \mathcal{S}_3} D^2f(X_t^x) (Y_t^{\sigma(l)}, Z_t^{\sigma(m), \sigma(n)}) \right]. \end{aligned}$$

Combining these formulas with the above statement gives

$$\begin{aligned} \|D\phi(t, x) \cdot h\| &\leq C\|h\|, \\ \|D^2\phi(t, x) (h, k)\| &\leq C\|h\|\|k\|, \\ \|D^3\phi(t, x) (l, m, n)\| &\leq C\|l\|\|m\|\|n\|. \end{aligned}$$

In other words, $\|D^i\phi(t, x)\|$ is bounded by some constant for any $0 < t \leq 1$. Thus, with a change of constant again, we get the desired result. \square

D Multi-Dimensional Problems

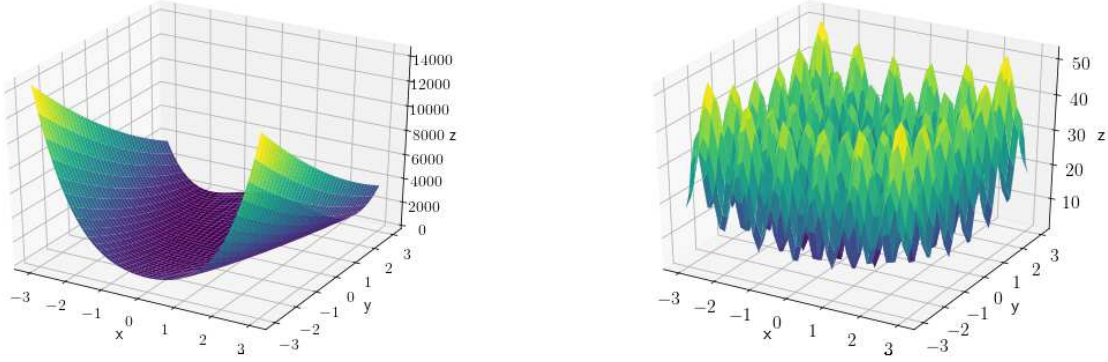
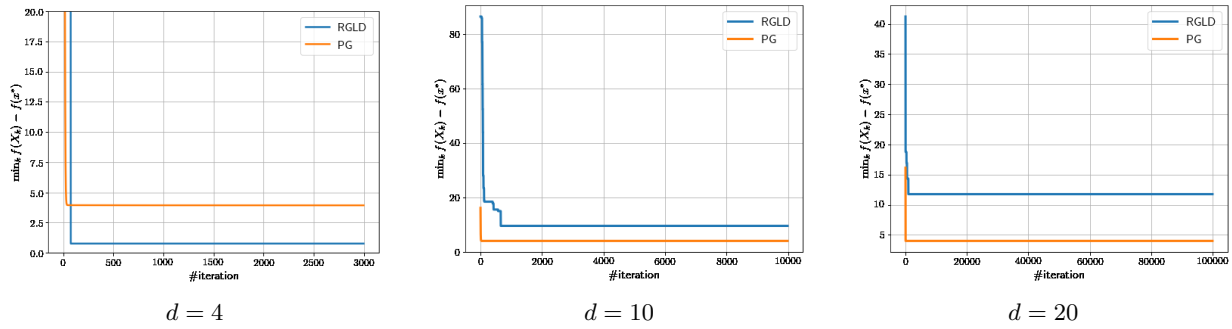
In this section, we demonstrate the performance of RGLD on classical non-convex test problems. In particular, we consider the Rosenbrock function (15) and Rastrigin function (16),

$$f(x) = \sum_{i=1}^{d-1} \{100(x_{i+1} - x_i^2)^2 + (1 - x_i)^2\}, \quad (15)$$

$$f(x) = 10d + \sum_{i=1}^d \{x_i^2 - 10 \cos(2\pi x_i)\}. \quad (16)$$

The feasible region of the Rosenbrock function is set to the region between a sphere of radius $0.5\sqrt{d}$ and one of radius $2\sqrt{d}$ centered at the origin, and that of the Rastrigin function is set to the region between a sphere of radius 0.9 and one of radius 5.12 centered at the origin. Figure 9 shows a 3D plot of each function. We can only show a 3D plot when $d = 2$, but the Rosenbrock function has two local minima when $d \geq 4$. It has a global minimum at $(1, \dots, 1)$, with $f(1, \dots, 1) = 0$, and a local minimum around $(-1, 1, \dots, 1)$, with $f(-1, 1, \dots, 1) = 4$. Meanwhile, the Rastrigin function has many local optima, which makes global optimization extremely challenging. It has a global minimum at $(0, \dots, 0)$, with $f(0, \dots, 0) = 0$.

Let us examine how RGLD optimizes these two functions under different dimensionalities. We scale β linearly with d according to our main theorem and generate the initial values randomly. Figure 10 shows the results for a constrained Rosenbrock function when $d = 4, 10, 20$. RGLD outperforms PG only when $d = 4$. When $d \in \{10, 20\}$, RGLD performs worse than PG, which always stagnates around 4. This is partly because the feasible region gets larger as d grows and it also implies that the curse of dimensionality affects RGLD, which may cause an explosion in iteration complexity. Figure 11 shows the results for constrained Rastrigin problems when $d = 2, 3, 5, 10, 20, 30$. All of the experiments fail to find the global minimum but the figure demonstrates that RGLD outperforms PG for small dimensionalities except $d = 10$. The failure at $d = 10$ is partly because the direction of the stochastic noise sometimes diverts away from deeper valleys or better local solutions.


 Figure 9: 3D plot of the objective function f when $d = 2$.

 Figure 10: Convergence of the iterates by PG and RGLD for constrained Rosenbrock problems. $\eta = 5 \times 10^{-4}$, $\beta = 0.25 \times d$. The initial values are randomly generated.

D.1 Dependence on Dimensionality

In this subsection, we arrange the plots above to visualize how higher dimensionality degrades performance. Figure 12 shows that, on the Rosenbrock problems, RGLD performs worse as d grows. Indeed, RGLD outperforms PG only when $d = 4$. We observe the same tendency on the Rastrigin function (Figure 12).

Convergence Error Analysis of RGLD

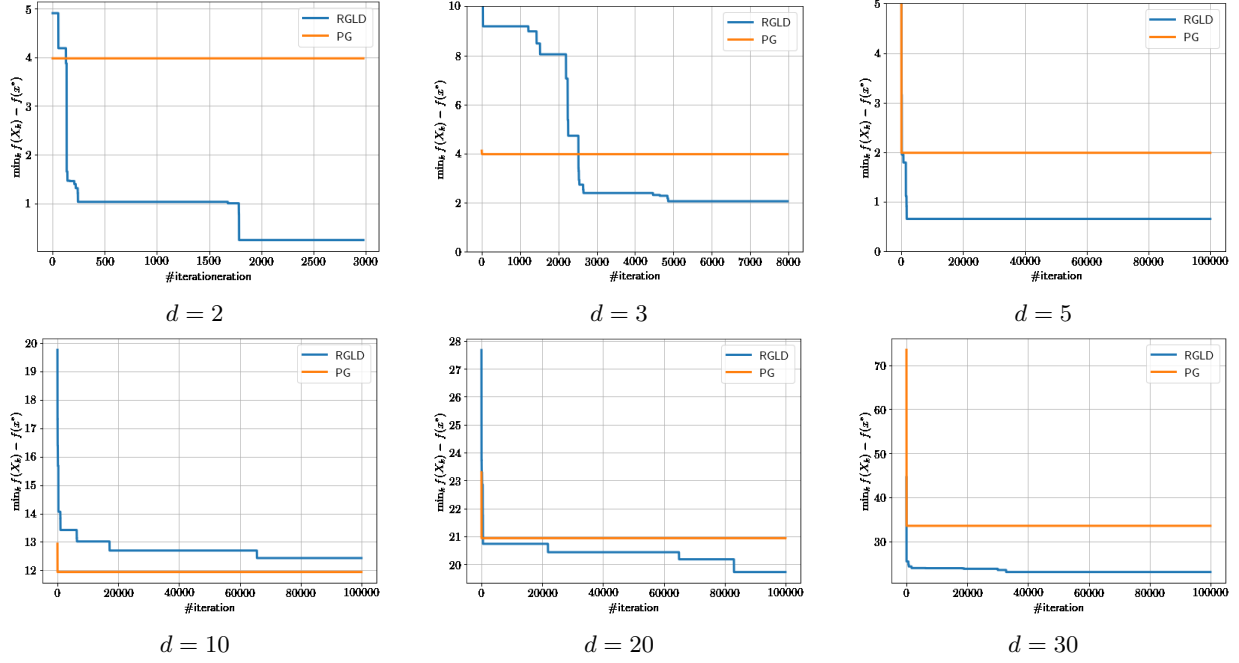


Figure 11: Convergence of the iterates by PG and RGLD for constrained Rastrigin problems. $\eta = 5 \times 10^{-4}$, $\beta = 0.05 \times d$. The initial values are randomly generated.

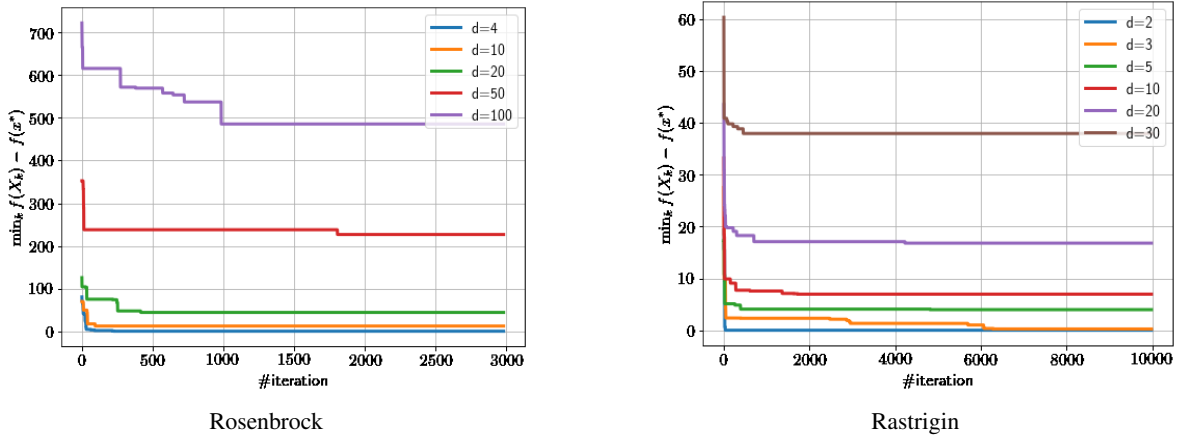


Figure 12: Convergence of the iterates by RGLD for constrained problems under different d .